

Scaling the robustness of the solutions for quantum controllable problems

S. Kallush¹ and R. Kosloff²¹*Department of Physics, ORT-Braude College, P.O. Box 78, 21982 Karmiel, Israel*²*The Institute of Chemistry, Hebrew University, 91904 Jerusalem, Israel*

(Received 27 April 2011; published 20 June 2011)

The major task in quantum control theory is to find an external field that transforms the system from one state to another or executes a predetermined unitary transformation. We investigate the difficulty of computing the control field as the size of the Hilbert space is increased. In the models studied the controls form a small closed subalgebra of operators. Complete controllability is obtained by the commutators of the controls with the stationary Hamiltonian. We investigate the scaling of the computation effort required to converge a solution for the quantum control task with respect to the size of the Hilbert space. The models studied include the double-well Bose Hubbard model with the SU(2) control subalgebra and the Morse oscillator with the Heisenberg-Weil algebra. We find that for initial and target states that are classified as generalized coherent states (GCSs) of the control subalgebra the control field is easily found independent of the size of the Hilbert space. For such problems, a control field generated for a small system can serve as a pilot for finding the field for larger systems. Attempting to employ pilot fields that generate superpositions of GCSs or cat states failed. No relation was found between control solutions of different Hilbert space sizes. In addition the task of finding such a field scales unfavorably with Hilbert space sizes. We demonstrate the use of symmetry to obtain quantum transitions between states without phase information. Implications to quantum computing are discussed.

DOI: [10.1103/PhysRevA.83.063412](https://doi.org/10.1103/PhysRevA.83.063412)

PACS number(s): 32.80.Qk, 02.30.Yy, 03.67.-a

I. INTRODUCTION

Quantum control (QC) focuses on guiding quantum systems from initial states to targets governed by time-dependent external fields [1,2]. Two interlinked theoretical problems dominate quantum control: controllability and inversion. Controllability addresses the issue of the conditions on the quantum system which enable control. The target could be either state-to-state control or a more difficult task of implementing a unitary transformation in a group of states. In closed Hilbert space the conditions for complete controllability have been addressed by Tarn and Clark [3–5]. In short, a system is completely controllable if the combined Hamiltonians of the control and system span a compact Lie algebra. Moreover, complete controllability implies that all possible unitary operators can be generated.

The task of inversion, finding a control field, for a control task still has to be addressed. The methods developed to solve the inversion problem could be classified as global, such as optimal control theory (OCT) [6–8], or local, e.g., local control [9–11]. OCT casts the inversion task into an optimization problem which is subsequently solved by an iterative approach. Local control inversion is based on guiding the system at each instant to the target employing local temporal conditions. Recently a generalization has been suggested to bridge the gap between the two approaches [12]. The task of inversion becomes more difficult when the size of the system increases. In the present study we want to classify the difficulty in state-to-state inversion according to the algebraic structure of the control Hamiltonian, and the nature of the initial and target states.

Typically the Hamiltonian of the system is divided into an uncontrolled part \hat{H}_0 and a control Hamiltonian composed from a subalgebra

$$\hat{H} = \hat{H}_0 + \sum_j \alpha_j(t) \hat{A}_j, \quad (1)$$

where $\alpha_j(t)$ is the control field for the operator \hat{A}_j and the set of operators $\{\hat{A}_j\}$ form a closed small Lie subalgebra. This model includes molecular systems controlled by a dipole coupling to the electromagnetic field. Complete controllability requires that the commutators of \hat{A}_j and \hat{H}_0 span the complete algebra $U(N)$ where $N = n^2 - 1$ and n is the size of the Hilbert space of the system. If \hat{H}_0 is part of the control algebra, the system is not completely controllable, i.e., there are state-to-state transitions which cannot be accomplished [3]. Specifically we study a scenario where the size of the subalgebra of control is constant but the size of the Hilbert space increases. It has recently been found [13] that if the control fields are subject to Markovian noise, complete state-to-state control is lost when the size of the Hilbert space increases. Under such a control Hamiltonian there are states which are relatively immune to noise, i.e., these are the generalized coherent states (GCSs) with respect to the control subalgebra [14]. The superposition states of GCSs are fragile and they become uncontrollable targets when the size of the system increases. Does this classification of states prevail when considering the task of inversion? Are state-to-state targets from a GCS to a GCS easier to obtain compared to a state composed from a superposition of GCSs?

A systematic study of the control landscape has been carried out by Rabitz *et al.* [15,16]. Based on the structure of unitaries, they found a generic landscape flat at the bottom and top and trap free for unrestricted state-to-state control problems. Trap-like saddle points seem to emerge for the more complicated control task of finding the field representation for unitary or nonunitary transformations [17]. The difficulty to converge to a solution was found to increase exponentially with the size of the system N , for the task of finding a field generating a unitary transformation [18,19]. A weaker dependence on N was found for a state-to-state task [20]. In a

recent study [21] such convergence properties were attributed to a large depth of the Lie algebra of the control Hamiltonian meaning that controllability is obtained after a long sequence of commutators of $\hat{\mathbf{H}}_0$ and $\hat{\mathbf{A}}$. It was found that for control Hamiltonians that couple distant states in the Hilbert space, the difficulty to achieve a solution depends weakly on the size of the system. These control problems were classified to have a small depth [21].

Typical algorithms of optimal control theory are iterative [6–8,19]. For large systems the convergence of OCT is fast in the first iterations but later saturates or becomes stagnant. Therefore, accurate solutions for large systems of the control problem are difficult to reach. A good initial guess for the control field can speed convergence considerably. Ideally, a control field of an easy-to-solve small quantum system could serve as a pilot initial guess for large quantum systems. In this paper we study the hypothesis of using such pilot fields and relate the results to the difficulty of inversion. This study explores two generic systems: the many-body Bose-Hubbard (BH) model, where the control Hamiltonian possesses the SU(2) subalgebra and the Morse oscillator, with the Heisenberg-Weil control algebra. The structure of this paper is as follows: Section II will present the models and the control schemes that will be employed. Section III will present the results for the BH and Morse oscillators, and Sec. VI will discuss the results in the context of applicability of quantum control to large systems.

II. FORMALISM AND MODELS

A. Bose-Hubbard model

First, we explore a many-body quantum system characterized by binary interactions between particles. The scaling of the Hilbert space is equivalent to the increase in the number of particles in the system. The two-mode Bose-Hubbard model [22] will be used for the demonstration. It is a model for an interacting Bose-Einstein condensate in a double-well potential [23]. The control task is to move particles from one well to the other. In addition, this model is one of the archetype systems to demonstrate quantum chaos.

The stationary Hamiltonian of BH one-dimensional double-well potential is given by

$$\hat{\mathbf{H}}_0 = -\Delta(\hat{\mathbf{a}}_1^\dagger \hat{\mathbf{a}}_2 + \hat{\mathbf{a}}_2^\dagger \hat{\mathbf{a}}_1) + \frac{U}{2}[(\hat{\mathbf{a}}_1^\dagger \hat{\mathbf{a}}_1)^2 + (\hat{\mathbf{a}}_2^\dagger \hat{\mathbf{a}}_2)^2], \quad (2)$$

which is the uncontrolled drift Hamiltonian. The $\hat{\mathbf{a}}_i$ are the annihilation operators for a particle in the i th well, Δ is the nearest-neighbor hopping rate, and U is the strength of the on-site interactions between particles. Using the fact that the total number of particles is conserved, this Hamiltonian can be reformulated employing angular-momentum operators of the SU(2) algebra. The control is obtained by shifting the energy bias between the two wells [23]. This leads to the control operator

$$\hat{\mathbf{J}}_z = (\hat{\mathbf{a}}_1^\dagger \hat{\mathbf{a}}_1 - \hat{\mathbf{a}}_2^\dagger \hat{\mathbf{a}}_2). \quad (3)$$

The control field $\mu(t)$ governs the energy balance between the two modes. The operators in the Hamiltonian (2) are transformed [24] to the SU(2) Lie-algebraic form leading to

$$\hat{\mathbf{H}} = -2\Delta\hat{\mathbf{J}}_x + U\hat{\mathbf{J}}_z^2 + 2\mu(t)\hat{\mathbf{J}}_z. \quad (4)$$

The $\hat{\mathbf{J}}_i$ are the operators for the projections of the angular momentum of the i axis, and the Hilbert space of the system of N bosons in this model corresponds to the $j = N/2$ irreducible representation of the SU(2) algebra. The addition of the nonlinear term $U\hat{\mathbf{J}}_z^2$ generates the complete controllability condition, since the commutators with the linear terms generate the full U(N) algebra. We choose the parameters $\Delta = 15$ and $U = 2\Delta/j$. The critical point of this one-dimensional system is obtained for $U = 2\Delta/j$ and $\mu = 0$. For these parameters the dynamics are chaotic. The quantum implication is that an initially localized state diverges rapidly and occupies the whole Hilbert space. According to the criteria of Moore *et al.* [21] this Hamiltonian has a large depth, since the Hamiltonian is banded along the diagonal.

We define the quality of state-to-state control at time T by the fitness $F = \langle \hat{\mathbf{P}} \rangle_{\psi_T}$, where $\hat{\mathbf{P}} = |\psi_T\rangle\langle\psi_T|$ is the target-state projection operator. The first step is to find the pilot field for which we seek a solution to the control problem for a small number of particles $j = N/2 \sim 10$. We will then explore the universality of the control field for increasing number of particles. Two methods are employed to generate the control field. The first method, optimal control theory, is based on Krotov's algorithm which guarantees monotonic convergence [6]. An iterative forward and backward propagation leads to convergence. The incremental correction to the field is proportional to

$$\Delta\mu(t) \propto -\text{Im}\langle\chi(t)|\hat{\mathbf{J}}_z|\psi(t)\rangle. \quad (5)$$

Here $|\psi(t)\rangle$ is the forward wave function with the initial state as its boundary and $|\chi(t)\rangle$ backward propagation starting from the target state. Alternatively, a local control (LC) strategy is applied to guarantee an instantaneously monotonic increase of the fitness with [9,10]

$$\mu(t) \propto \text{Im}\langle\hat{\mathbf{P}}\hat{\mathbf{J}}_z\rangle_{\psi(t)}. \quad (6)$$

The control problem is characterized by the free propagation of the drift Hamiltonian $\hat{\mathbf{H}}_0$. The analysis is based on the generalized coherent states with respect to the SU(2) subalgebra. The GCSs minimized uncertainty with respect to the generators of the SU(2), which is equivalent to maximizing the generalized purity $p_{\text{gen}} = \langle\hat{\mathbf{J}}_x\rangle^2 + \langle\hat{\mathbf{J}}_y\rangle^2 + \langle\hat{\mathbf{J}}_z\rangle^2$. In addition the GCSs are invariant to unitary transformations generated by the SU(2) subalgebra. The generalized purity p_{gen} characterizes the locality of the state in phase space. For the parameters chosen, an initially localized state (GCS) will spread rapidly over the whole phase space. Under these chaotic conditions the generalized purity decreases rapidly. For other ratios between U and Δ/j , classical-like solutions emerge for the GCS where the purity is almost constant during the evolution. The quantum dynamics can be solved by direct propagation up to $j = 10\,000$ and approximately up to $j = 10^6$ [14].

B. Morse oscillator control

The drift Hamiltonian for this system $\hat{\mathbf{H}}_0$ in Eq. (1) is the well-known nonlinear Morse oscillator:

$$\hat{\mathbf{H}}_0 = \frac{\hat{\mathbf{p}}^2}{2m} + D_e[(1 - e^{-\alpha\hat{\mathbf{x}}})^2 - 1], \quad (7)$$

where m is the particle mass, D_e is the dissociation energy, and α determines the spatial extent of the potential. The number of bound energy states or the size of Hilbert space is altered by changing the value of \hbar , leaving all the other parameters unchanged. The control Hamiltonian consists of the Heisenberg-Weil operators $\hat{\mathbf{x}}$ and $\hat{\mathbf{p}}$ where coherent states constitute the GCSs which have minimum uncertainty with respect to the generators of the algebra.

$$\hat{\mathbf{H}} = \hat{\mathbf{H}}_0 + \alpha_x(t)\hat{\mathbf{x}}. \quad (8)$$

Note that both of the models that are considered here could be classified as weakly connected Hamiltonians according to [21]. Exponential scalability is expected to emerge with the increase of the Hilbert space. It is important to mention that the typical large systems in quantum control, such as spin chains and molecular vibrational manifolds, fall into this category. The time-dependent Schrödinger equation was integrated using the Chebyshev propagator [25], and the states were represented employing a Fourier grid.

III. RESULTS

A. BH model: General size dependency

The initial state of the first control task is a GCS $|j\rangle$ corresponding to all particles in the left well. The control objective is to generate the ground state of the system in which $\langle \hat{\mathbf{J}}_z \rangle = 0$, and both of the wells are equally occupied. Note that the generalized purity of the ground state of the system depends on the parameters. Its purity goes to unity as j and U increase, and the ground state becomes local in the Hilbert space.

The OCT procedure is initiated from a structureless initial control field. Figure 1 displays the increase of the fitness with the number of OCT iterations for various values of j , on a logarithmic scale. Observing Fig. 1, it is clear that difficulty

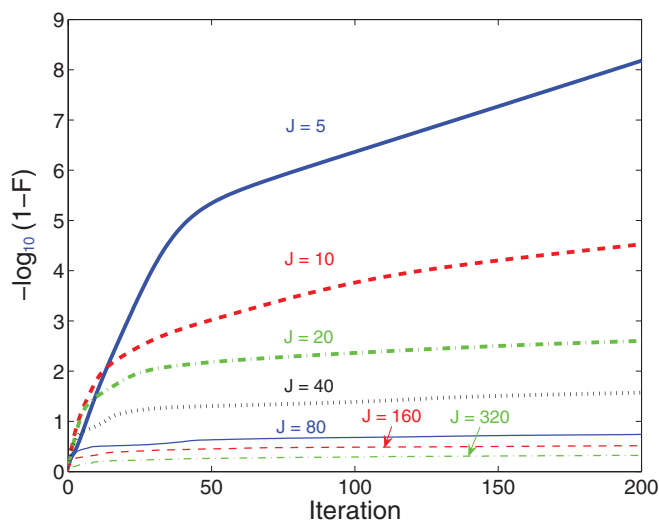


FIG. 1. (Color online) Fitness vs the Hilbert space size obtained by OCT: deviation from unity fitness vs the number of iterations, for different j values. Initial GCS state: $\langle \hat{\mathbf{J}}_z \rangle = j$, all the particles in one of the wells. The target is the ground state of the system. Initial guess for all the optimization is taken as $\mu(t) = 10 \sin(25t\pi/T)$.

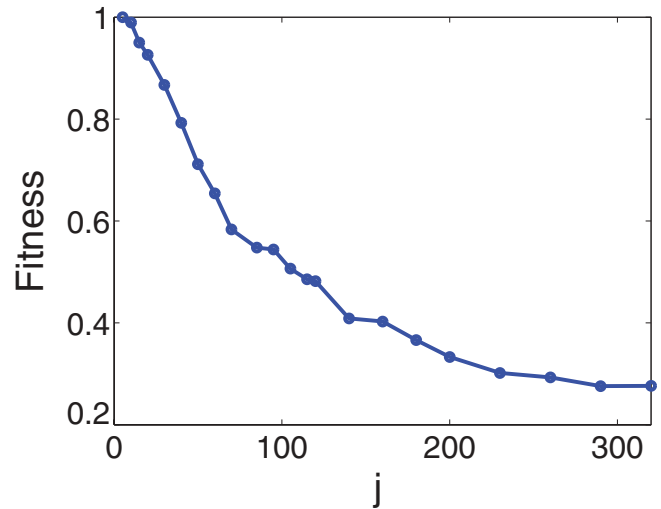


FIG. 2. (Color online) Fitness at the 200th iteration vs j . The control task is identical to that in Fig. 1.

to converge to a fitness of unity increases exponentially with the size of the Hilbert space. Figure 2 displays the fitness after 200 iterations versus j demonstrating monotonic decrease.

Figure 3 presents the temporal generalized purity for small and large Hilbert spaces. The decrease in generalized purity means that the temporal wave function spreads to a superposition of many GCS states before it reassembles to reach the final target. The decrease of the generalized purity is recoverable for $j = 5$, but not for $j = 320$. This result is expected for the BH model, which can be classified as a weakly connected Hamiltonian.

B. Can the search for the optimal field be guided by the scalability of the SU(2) algebra?

To test this hypothesis the optimal field of the $j = 5$ solution (with fitness of 0.99) is used for an initial pilot guess for

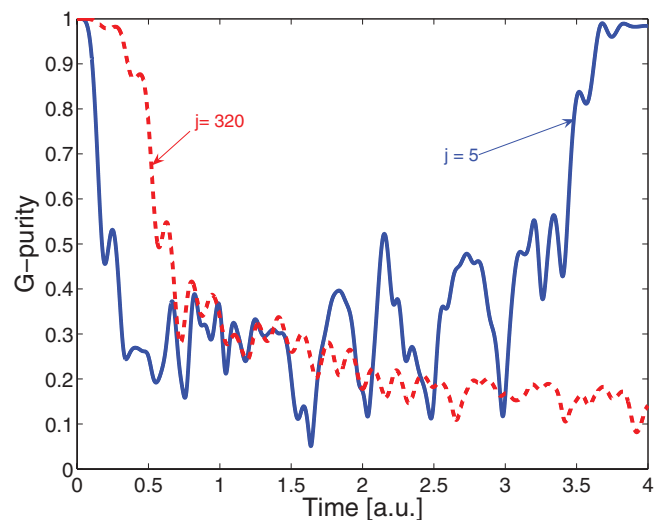


FIG. 3. (Color online) Generalized purity vs time for $j = 5$ (solid blue) and $j = 320$ (dashed red), for the control task of Fig. 1, after 200 iterations. The generalized purity is defined with respect to projection on the SU(2) subalgebra. The period of the motion is $2\pi/\Delta = 0.42$.

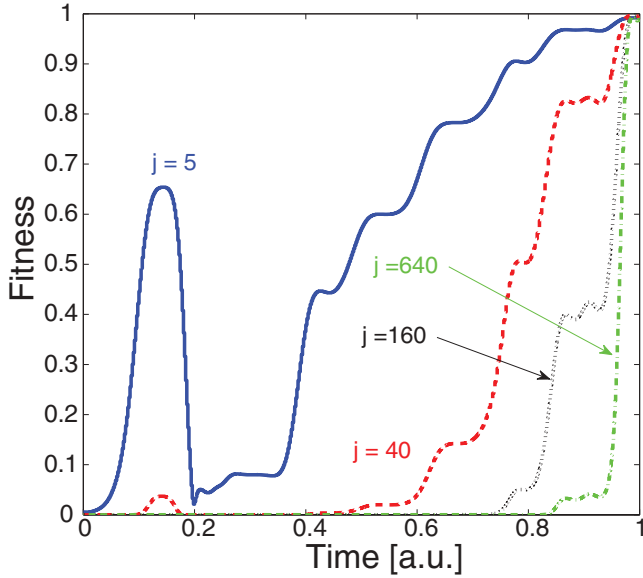


FIG. 4. (Color online) Temporal fitness values for different j values; the pilot field was the optimal solution of $j = 5$. Different curves correspond to different j values.

larger j . Figures 4 and 5 present the temporal fitness and purity for the optimized solution for various j values, starting with the optimal control field of $j = 5$. A close-to-unity of fitness was achieved in all cases. An explanation is suggested by inspecting the dynamics of the expectation values of the SU(2) subalgebra which are almost identical for different j (see Fig. 6). Another indication is the high value of purity in all cases during the evolution. The mechanism of the control process under the OCT formalism is to preserve the localized GCS state during the dynamics. Then, at the very last steps of the dynamics, it pushes the state toward the target, in a period that will avoid the spread of the wave function due to the nonlinear

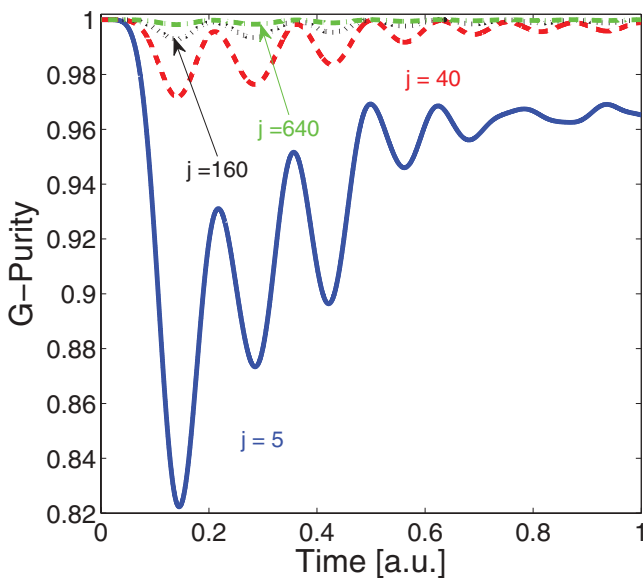


FIG. 5. (Color online) Generalized purity vs time for different j values, for a converged field starting from the pilot field generated from the optimal solution of $j = 5$.

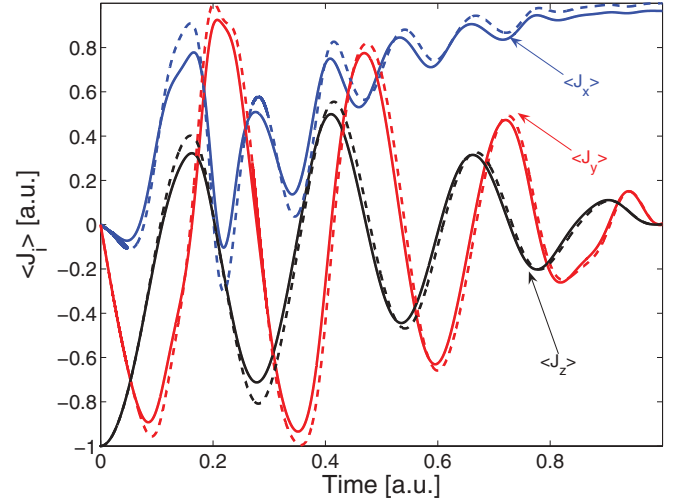


FIG. 6. (Color online) Expectation values $\langle \hat{J}_x \rangle$, $\langle \hat{J}_y \rangle$, and $\langle \hat{J}_z \rangle$ vs time for $j = 5$ and $j = 160$, in solid and dashed lines, respectively. The close resemblance indicates that both states are GCSs.

term in Eq. (4). The early period of the dynamics is therefore redundant, and the goal could be reached in shorter period T , where the lower limit is determined by the uncontrolled drift terms in the Hamiltonian, $T \sim 2\pi/\Delta$.

C. Can other control solutions serve as a pilot guess for larger systems?

For this task we examine the direct optimization formalism of local control, which is a noniterative and unidirectional approach. Figure 7 presents the temporal fitness for $j = 5$ in the blue line, obtained from a local control strategy. The fitness increases monotonically in time, a direct consequence of the LC formalism. Note that OCT reaches almost unity

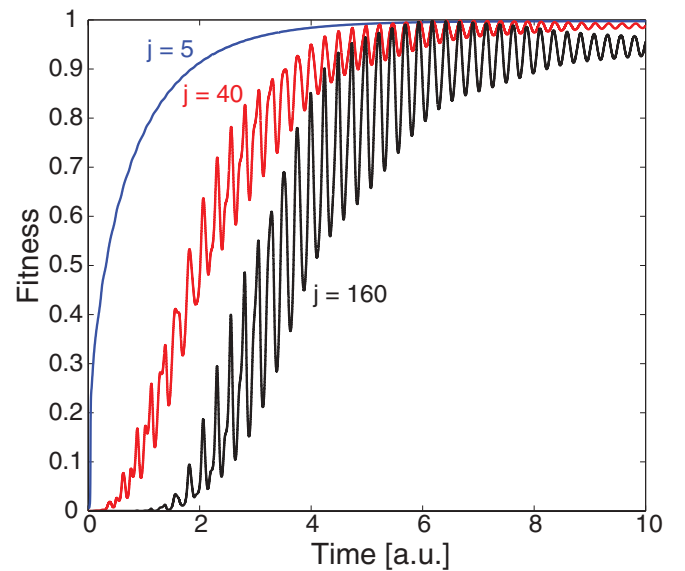


FIG. 7. (Color online) Fitness vs time for local control. Optimization for $j = 5$, solid curved line. The fitness for $j = 40$ and 160, using the pilot $j = 5$ field, are plotted in grey (red) and black lines, respectively.

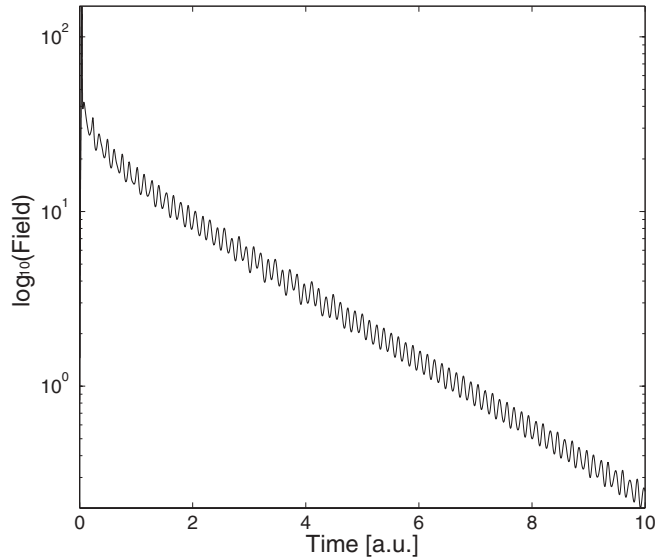


FIG. 8. Control field from local control, in logarithm scale. The OCT corrected field is very similar (not plotted).

of fitness in a shorter period. The control field plotted in Fig. 8 can be decomposed to a dominant single frequency with exponentially decaying amplitude. Through the process the purity is very close to unity and thus the dynamics could be described in terms of a single GCS at all times.

For large j , local control fails. A possible reason is an increasing demand for accurate timing countering the tendency of the system to become uncontrollable. This can be associated with the reduction in purity for larger systems with high j . Nevertheless, the pilot field can be used to overcome this difficulty. The grey (red) and black curves in Fig. 7 display the fitnesses for $j = 40$ and 160 , with the pilot field optimized for $j = 5$. The monotonic convergence was not followed, although the general trend of increasing fitness is still valid. Figure 9 presents the temporal fitness after an additional single OCT

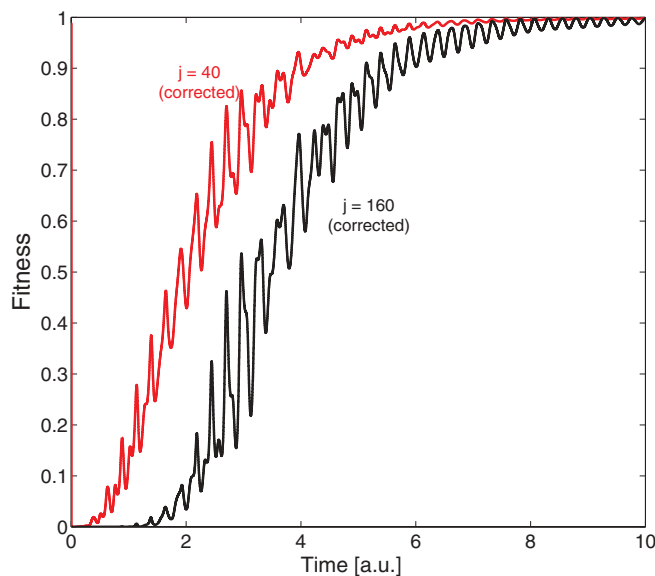


FIG. 9. (Color online) Fitness vs time for local control with a field corrected by a single OCT iteration.

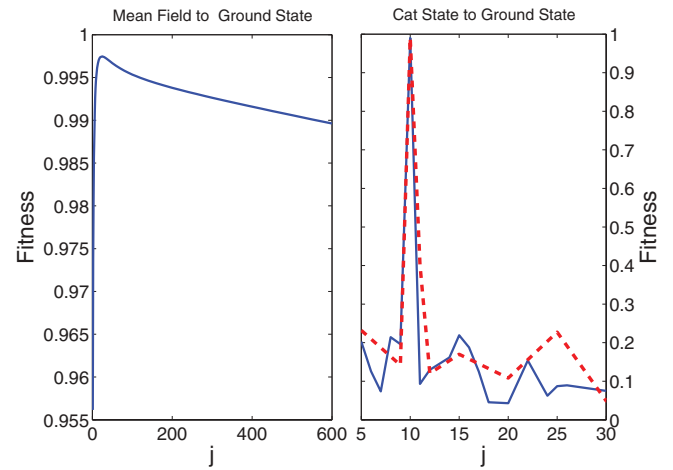


FIG. 10. (Color online) Fitness vs j for a ground-state target state. Left: Initial GCS: all the particles in one of the wells $|\psi(0)\rangle = |j\rangle$. Right: Initial cat state: $|\psi(0)\rangle = \frac{1}{\sqrt{2}}(|j\rangle + |-j\rangle)$. The dashed line in the right panel corresponds to the inverse GCS to cat state transition. In all cases the field was optimized for $j = 10$.

iteration used to find the minor adjustments that are required to reach a converged solution. This field was tested also for $j = 20\,000$ using the STNLSE algorithm [26]. The solution obtained by the combined LC and OCT method was found to be adequate for this large system. To generalize, if the initial and final target states are localized GCSs, a scalable pilot guess field obtained either by OCT or by LC for small j leads to a final state which is very close to the target for larger j . The purity conserving fields that were found are robust solutions of the control problem, irrespective of the size of the system.

D. Can the pilot field be generalized to arbitrary initial and final states?

An obvious generalization would define the target or initial state as superposition of GCSs, a Schrödinger cat state. Figure 10 compares the fitness of two kinds of tasks as a function of j generated from the pilot field optimized for $j = 10$. The target state for both cases was the ground state of the system. In the left panel, the initial state is a GCS $|\psi(0)\rangle = |j\rangle$ for which the fitness is a smooth function of j , and remains close to unity even when the size of the system is enlarged by a factor of 60. In the right panel, the initial state is a cat state $|\psi_{\text{cat}}\rangle = \frac{1}{\sqrt{2}}(|j\rangle + |-j\rangle)$, with zero purity. For such tasks, we find no correspondence between the optimal field and fitness of different j values. Moreover, no correlation was found between the solutions for two adjacent j values.

E. Can symmetry be employed to generate a cat state?

It seems that scalable control for weakly connected Hamiltonians is only possible for target and initial states which are GCSs. Moreover, real experiments which involve control of the linear $\{\hat{J}_i\}$ set of operators are accompanied by unavoidable noise that will erase all the long-term coherences and evolve the system into a classical mixture of GCSs [13]. Nevertheless, the symmetry of the system could be exploited in some cases

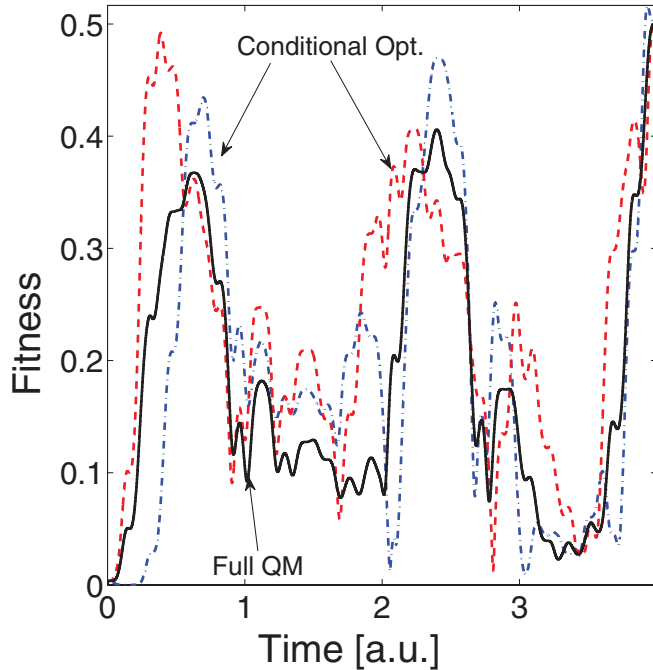


FIG. 11. (Color online) Conditional optimization. Fitness vs time for the conditional optimization of the half cat states $\frac{1}{\sqrt{2}}|j\rangle$ and $\frac{1}{\sqrt{2}}|-j\rangle$, in blue dashed-dotted and red dashed lines, respectively. (solid) Fitness/2 vs. time for the cat state. In all of the cases here $J = 5$.

to achieve the right relative phase between components of the target wave function. Such an example is demonstrated in Fig. 11.

A conditional OCT optimization was performed to find the common field that stirs each of the components of the cat state $|\psi_{\text{cat}}\rangle$ toward the ground state of the system. The optimization was performed *in parallel*, and no phase information was interchanged between the two optimizations. The dashed and dotted-dashed lines of Fig. 11 represent the temporal fitness for each of the components for the converged field. The control field is able to drive the maximal overall target amplitude from each of the individual components. However, due to time reversal symmetry, the final states contain components orthogonal to the target state. That is, if a similar field can take two states into identical state then the inverted dynamics are indeterministic.

Applying the optimal field on the cat-state superposition achieves the goal of unity purity and fitness with the target GCS. The orthogonal components with the target interfere destructively. The correct phase relation between the two components of the state is a consequence of the symmetry of the Hilbert space. Violation of the phase relation for cat states appears only when a break of the symmetry takes place, i.e., $|\psi_{\text{cat}}^{NB}\rangle \propto c_{\text{left}}|j\rangle + c_{\text{right}}|-j\rangle$, with $c_{\text{left}} \neq c_{\text{right}}$. Figure 12 presents the phase relation between the two components as a function of the ratio $c_{\text{right}}/c_{\text{left}}$. The dependency is smooth and quadratic. In the general case, erasure of the phase information due to noise will avoid the construction of superpositions of GCSs, especially for large systems. Nevertheless, transitions between targets and initial states that fit the phase relation that

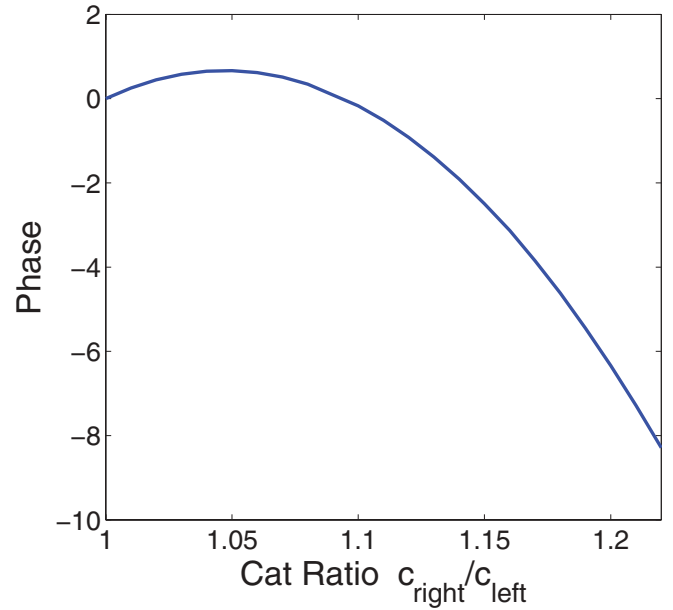


FIG. 12. (Color online) Relative phase of the cat state's components vs the ratio of the amplitude between the components. In all of the cases here, $J = 5$.

emerges from the symmetry of the Hilbert space are feasible experimentally.

F. Morse oscillator

The same concepts are now applied to the example of the controlled Morse oscillator. The initial state was chosen as a shifted coherent state or a cat state, i.e., superposition of well-separated coherent states. The target was the ground state of the oscillator. The solutions for the two kinds of control tasks was tested with a varied size of Hilbert space, while maintaining the coupling scheme. This is achieved by changing the value of the effective \hbar in the dynamics. Note that in the current context the states with lowest uncertainty with respect to the Heisenberg-Weil algebra defining the generalized coherent states are the (classical) coherent states. A decrease of \hbar corresponds to a shift to classical dynamics and a higher density of states. The applied pilot field was obtained from the solution of the control problems with $\hbar = 1$, $m = 10$ a.u., $D_e = 40$ hartree, and $\alpha = 1.5$ bohrs $^{-1}$. For these parameters, there are 20 bound states. A Fourier grid size of 128 was used for the simulation, and the same grid was used throughout the study. The classical period of motion corresponding to the bottom of the well is given by $\tau = 2\pi/\alpha\sqrt{m/2D_e} \approx 1.5$.

Four examples are demonstrated in Fig. 13. The fitness vs \hbar for the task of taking a coherent state located at $\delta x = 0.15$ bohrs into the ground state of the system ($\delta x = 0.03$), is depicted by a solid black line. The target time for the transition $T = 1.66 \approx \tau$ ensures a minimal decrease in the purity of the state. The solution conserves high fitness for a wide range of system sizes. In the dashed blue line, the same task is examined but now for a longer target time $T \approx 20\tau$. The larger propagation time allows the wave function to spread during the dynamics, and the solution's robustness is diminished but still significant. The dotted-dashed red and dotted green lines

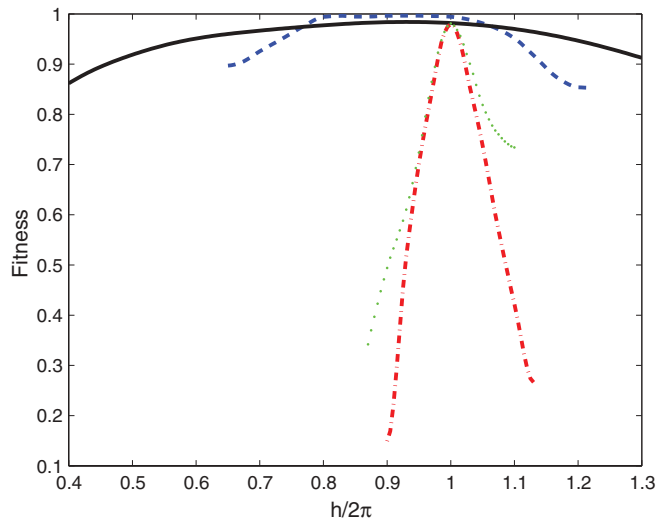


FIG. 13. (Color online) Fitness for a control using a pilot field generated for $\hbar = 1$ for the Morse oscillator. Solid black line: fitness vs \hbar for a coherent-state to ground-state transition. Target time $T \approx \tau$. At dashed blue line: the fitness for $T \approx 20\tau$. The dashed-dotted red and dotted green lines represent the fitness for transforming a superposition of two coherent states to the ground state, in the case of low and high initial energy of the superposition, respectively.

represent the fitness for a difficult control task, generating the ground state from a superposition of two coherent states with inverse phase $|\psi_{\text{cat}}\rangle = |\alpha\rangle - |-\alpha\rangle$, for $\alpha = 0.02$ and $\alpha = 0.32$ bohrs. The enhancement of convergence due to the pilot field is extremely limited, and the difference between the initial superposition is not significant. Note that for this nonlinear system a cat state can be generated from the ground state by first generating a shifted coherent state. At a second step the drift nonlinear Hamiltonian \hat{H}_0 will generate a cat state after a period which is half the revival time. This time, however, is long compare to T , the current control target time.

IV. OUTLOOK

The difficulty in converging a control field to generate state-to-state transitions can be related to the algebraic structure of the control Hamiltonian. When the initial and final states are generalized coherent states of the control algebra, then a pilot field of a small Hilbert size leads to fast convergence when the size of the Hilbert space increases. This is not so when the initial or target states are superpositions of generalized coherent states. It seems that no relation exists between the control fields of such targets for different Hilbert space sizes.

The generalized coherent states or GCSs maximize the generalized purity with respect to the control algebra; therefore they are considered the most “classical-like” localized states. The control of such states is achieved by maintaining high generalized purity for all times. These control fields supply good control even when the system size increases.

The second category showed no scalable features of the field. This means that in this $U(N)$ system the task of generating a quantum compiler [18], translating an arbitrary unitary transformation to a control field, will scale unfavorably with system size. The present observations are consistent with the finding that noise on the control fields will completely degrade the control of superpositions of GCS. This noise will transform any superposition of GCSs into a mixture [14] thus destroying complete controllability. It seems that control fields that are required to generate superpositions of GCSs are intricate. As a result they are hard to find and are also extremely sensitive to noise.

ACKNOWLEDGMENTS

We thank Michael Khasin for sharing his insights. We gratefully acknowledge financial support from the Israel Science Foundation. The Fritz Haber Center is supported by the Minerva Gesellschaft für die Forschung GmbH München, Germany.

- [1] P. W. Brumer and M. Shapiro, *Principles of the Quantum Control of Molecular Processes* (Wiley Interscience, New York, 2003).
- [2] S. A. Rice and M. Zhao, *Optical Control of Molecular Dynamics* (Wiley, New York, 2000).
- [3] J. Clark and T. Tarn, *J. Math. Phys.* **24**, 2608 (1983).
- [4] C. Lan, Q. Chi, T. Tarn, and J. Clark, *J. Math. Phys.* **45**, 052102 (2005).
- [5] V. Ramakrishna and H. Rabitz, *Phys. Rev. A* **54**, 1715 (1996).
- [6] D. J. Tannor, V. Kazakov, and V. Orlov, in *Time Dependent Quantum Molecular Dynamics*, NATO Advanced Study Institute, Series B: Physics, Vol. 299 (Plenum, New York, 1992).
- [7] S. Shi and H. Rabitz, *J. Chem. Phys.* **95**, 1487 (1991).
- [8] A. Bartana, R. Kosloff, and D. Tannor, *J. Chem. Phys.* **106**, 1435 (1997).
- [9] R. Kosloff, A. D. Hammerich, and D. Tannor, *Phys. Rev. Lett.* **69**, 2172 (1992).
- [10] R. S. Judson and H. Rabitz, *Phys. Rev. Lett.* **68**, 1500 (1992).
- [11] V. Engel, C. Meier, and D. J. Tannor, in *Advances in Chemical Physics*, edited by S. A. Rice, Vol. 141 (Wiley, New York, 2009).
- [12] T. S. Ho and H. Rabitz, *Phys. Rev. E* **82**, 026703 (2010).
- [13] M. Khasin and R. Kosloff, *Phys. Rev. Lett.* **106**, 123002 (2011).
- [14] M. Khasin and R. Kosloff, *Phys. Rev. A* **81**, 043635 (2010).
- [15] K. Moore, M. Hsieh, and H. Rabitz, *J. Chem. Phys.* **128**, 154117 (2008).
- [16] H. Rabitz, M. Hsieh, and C. Rosenthal, *Science* **303**, 998 (2004).
- [17] T. S. Ho, J. Dominy, and H. Rabitz, *Phys. Rev. A* **79**, 013422 (2009).
- [18] J. P. Palao and R. Kosloff, *Phys. Rev. Lett.* **89**, 188301 (2002).
- [19] J. P. Palao and R. Kosloff, *Phys. Rev. A* **68**, 062308 (2003).
- [20] T. Caneva, M. Murphy, T. Calarco, R. Fazio, S. Montangero, V. Giovannetti, and G. E. Santoro, *Phys. Rev. Lett.* **103**, 240501 (2009).
- [21] K. W. Moore, R. Chakrabarti, G. Riviello, and H. Rabitz, *Phys. Rev. A* **83**, 012326 (2011).
- [22] G. D. Mahan, *Many-Particle Physics* (Springer, New York, 2000).
- [23] S. Levy, E. Lahoud, I. Shomroni, and J. Steinhauer, *Nature (London)* **449**, 579 (2007).
- [24] A. Vardi and J. R. Anglin, *Phys. Rev. Lett.* **86**, 568 (2001).
- [25] R. Kosloff, *Annu. Rev. Phys. Chem.* **45**, 145 (1994).
- [26] M. Khasin and R. Kosloff, *Phys. Rev. A* **78**, 012321 (2008).